Open-ended coaxial probe measurements of complex dielectric permittivity in diesel-contaminated soil during bioremediation

Available online at www.sciencedirect.com

ScienceDirect

IFAC PapersOnline CONFERENCE PAPER ARCHIVE

IFAC PapersOnLine 59-30 (2025) 929–934

Statistically Refined Hysteresis Modeling in High-Nickel-Ternary-Cathode Cells ⋆

Aleksandar Dejanovic * **Marcelo Miranda Camboim** ** **Angelo Bonfitto** *** **Alfredo Primon** **** **S.M.Mahdi Alavi** † **Yasaman Masoudi** ‡ **Ofelia A. Jianu** *

* *Department of Mechanical, Automotive and Materials Engineering University of Windsor, Windsor, Canada (e-mail: dejanov@uwindsor.ca, ofelia.jianu@uwindsor.ca)*
** *C.A.A.R. do Brasil (e-mail: marcelo.camboim@external.stellantis.com)*
*** *Department of Mechanical and Aerospace Engineering, Center for Automotive Research and Sustainable Mobility (CARS), Politecnico di Torino, 10129 Torino, Italy (e-mail: angelo.bonfitto@polito.it)*
**** *Centro Ricerche Fiat S.C.p.A, 10043 Orbassano (TO), Italy (e-mail: alfredo.primon@crf.it)*
† *FCA Canada Inc, Windsor, ON, Canada (e-mail: mahdi.alavi@stellantis.com)*
‡ *FCA US LLC, Auburn Hills, Michigan, US (e-mail: yasaman.masoudi@stellantis.com)*

Abstract
A battery management system (BMS) relies on accurate battery models to perform predictions, where, equivalent circuit models (ECMs) are most practical. However, batteries possessing significant hysteresis cannot be effectively modeled with conventional ECMs, limiting BMS accuracy. Therefore, this study improves ECM accuracy by addressing hysteresis, a key lithium-ion (Li-ion) cell characteristic. In this context, a second-order Thevenin ECM, incorporating dynamic and instantaneous hysteresis was developed and tested on high-nickel-ternary-cathode (HNTC) Li-ion cells. When working with hysteresis models, the hysteresis tuning rate, γ, is an estimated parameter often defined as a constant and is overlooked in adjusting the rate of hysteresis decay. In the ECMs of this work, a variable gamma was identified and examined for different state of charge (SOC) intervals and temperatures. An n-way analysis of covariance (ANCOVAN) was applied to the variable response of gamma and indicated a significant gamma-hysteresis voltage relationship for specific SOC windows. Comparatively through validation of dynamic and total hysteresis modeling, results also indicate that incorporating instantaneous hysteresis does not necessarily improve overall model performance.

Keywords: Grey box modeling, Time-invariant systems, Hysteresis modeling, Energy systems, Complex systems.

1. INTRODUCTION

A reliable battery pack depends on the battery management system (BMS) to accurately estimate the battery state of charge (SOC) (Plett, 2004; Lin et al., 2017; Tekin and Karamangil, 2024). A common strategy to develop battery control algorithms is the use of equivalent circuit models (ECMs), empirical representations of a working lithium-ion (Li-ion) cell that are derived from common circuit elements (Plett, 2015; Tran et al., 2021; Naseri et al., 2022). The benefit of this strategy is the low computational cost and adequate resolution it provides for managing Li-ion cells (Plett, 2015; Lipu et al., 2021; Biju and Fang, 2023).

Several ECM structures are applicable to a Li-ion cell (Tran et al., 2021; Biju and Fang, 2023; Nozarijouybari and Fathy, 2024), where an accurate strategy to estimate the true state is critical to its performance and longevity (Christophersen, 2015). Hence, an accurate ECM must describe open circuit voltage (OCV) as a function of the state of charge (SOC), high-order polarization (or relaxation) voltages, internal voltage drop and gain, and depending on the cell, a less commonly described feature identified as hysteresis (Anton Van der Ven, 2022).

Hysteresis is a characteristic of secondary cells. The voltage of a Li-ion cell will deviate from its "true" OCV depending on whether it was previously charged or dis-

⋆ This work was supported by Mitacs through the Mitacs Accelerate International program (with Stellantis), and by the Ontario Graduate Scholarship. I would like to acknowledge Marcelo Miranda Camboim for equal contributions to this work. Yasaman Masoudi and Dr. Ofelia A. Jianu for equal contributions in supervising and managing the project.

10.1016/j.ifacol.2025.12.358

charged. Identifying and addressing this characteristic in an ECM has shown to improve the accuracy of the model and, consequently, its ability to enhance SOC estimation (Plett, 2015; Hodakovska et al., 2024). In Li-ion cells, the most prevalent anode material is graphite (Cheng et al., 2021) where major hysteresis bounds are minimal and often not addressed in standard graphite-anode cell models. Nevertheless, studying this phenomenon is increasingly vital, as a major target of the US Department of Energy Battery500 Consortium is a high specific energy upwards of 500Wh/kg (Whittingham, 2019) achievable with a high nickel content and silicon-doped anodes, a combination that usually presents significant hysteresis. In this context, the present work addresses the hysteresis phenomenon with the goal of improving the accuracy of a battery ECM.

The goals and contributions of this work explore the applicability of the hysteresis tuning rate, γ, for selected SOC windows to better describe the hysteresis observed in high-nickel-ternary-cathode (HNTC) cells at various temperatures. The improved accuracy, brought about by implementing hysteresis, for first (1RC) and second (2RC) orders ECMs are validated. The statistical significance of hysteresis voltage and SOC interactions on a variable tuning rate response is proven by a n-way analysis of covariance (ANCOVAN). Additionally, results suggest that augmentation of the model to describe instantaneous changes with a variable tuning rate is not statistically significant for the hysteresis voltage factor for all models. Validation supports these findings, demonstrating that a suitable one-state model should be selected considering model order and temperature.

The present work is structured as follows: Section 2 summarizes the observed phenomenon of hysteresis in Li-ion cells. Section 3 justifies implementing the one-state model for describing hysteresis in ECMs, and how the variable tuning rate and instantaneous parameters are incorporated for a 2RC model. Section 4 details the methodology. Section 5, discusses the results. Section 6 presents conclusions.

2. HYSTERESIS

The intrinsic presence of hysteresis in Li-ion cells is not well understood and imposes limited accuracy in SOC estimation by BMS. The author in (Anton Van der Ven, 2022) provides a detailed exploration of hysteresis in electrochemical systems. The study explains the mechanisms of hysteresis, focusing on first-order phase transitions during lithiation and delithiation. These transitions require overpotentials, leading to polarization and energy loss, represented by a hysteresis loop in the voltage profile. The work of (Akhilash et al., 2021) and (Murdock et al., 2021) discusses the chemical and/or physical properties that affect ion transport and therefore lead to hysteresis in Li-ion cells. The phenomenon is sensitive to electrical, thermal, and mechanical abuse and is inherent to HNTC cells. Hysteresis causes the OCV-SOC characteristic to correspond to more than one possible output for a given window ΔSOC, as shown in Figure 1. A cycle under the same conditions (e.g. constant temperature) is represented by two separate paths where charging is the direction of increase of SOC and discharging is the direction of decrease

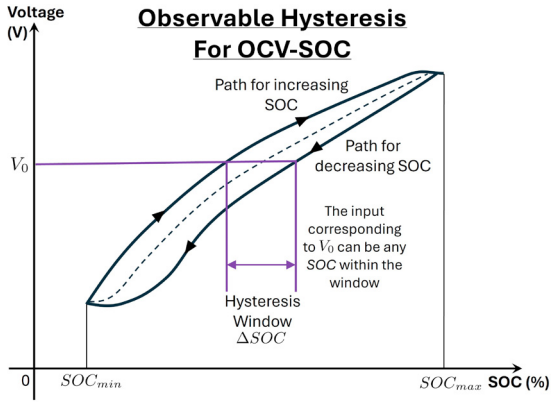

Figure 1. The property of hysteresis for a major loop which is considered to be one cycle for the path of increasing SOC to its maximum and a return path of SOC decreasing to its minimum.

of SOC. Assuming a maximum amplitude of the hysteresis bounds may be obtained from a major loop cycle, the percent error due to hysteresis ϵ_{hyst} can be calculated as follows:

$$\epsilon_{hyst} = \left| \frac{\Delta SOC}{SOC_{max} - SOC_{min}} \right| \times 100\% \qquad (1)$$

where the maximum amplitude of the hysteresis cycle is the range of inputs that could possibly lead to the same output of SOC. In (1), $SOC_{\max}$ and $SOC_{\min}$ denote the maximum and minimum SOC levels, respectively, which could be different from 100% and 0% depending on the design requirements. The terms charging (forward) and discharging (reverse) are denoted separately with respect to the SOC. A trivially simple solution to the problem of hysteresis is to take the midpoint between both curves as the average approximation, which gives rise to estimation errors for any given window depending on the severity of the presence of hysteresis voltages. This midpoint is represented as a line that subtends both upper and lower curves in Figure 1.

3. ONE-STATE MODEL OF HYSTERESIS

3.1 Selection of Hysteresis Model

The selection of a mathematical model to describe hysteresis is largely dictated by the application, accuracy, complexity, and availability of data. Some classical approaches which have seen several iterations and adaptions used in the study of hysteresis in other systems are the Preisach model, Krasnosel'skii-Pokrovskii (KP) model, Prandtl-Ishlinskii (PI) model, Maxwell-Slip model, Bouc-Wen model, and the Duhem model.

These models can be classified into operator-based or differential-based models (Hassani et al., 2014). The Preisach model is the most used operator-based model in battery applications, where KP and PI are subsets of it (Chayratsami and Plett, 2019). Despite the use of the operator-based models mentioned, they suffer in their application, complexity, and data availability. To perform effectively, they require extensive experimental data for parameterization (Hassani et al., 2014). The drawback is that these models require considerable computation to

implement for the best estimation performance in practice (Chayratsami and Plett, 2019).

Among the numerous models and strategies to account for the dynamic properties identified in Li-ion cells, the differential-based one-state model implemented by (Plett, 2015) was investigated. This is a computationally simple empirical model, but the implementation of such a model has demonstrated its effectiveness in improving the accuracy of the ECM calibration framework by integrating a model that directly accounts for hysteresis.

3.2 State-Space Representation of the Model

The electrochemical behaviour of the cell can be modeled provided current, voltage and temperature measurements at the terminals. To effectively capture the observed response, the ECM is calibrated with data from precise lab test data. This model does not represent the physical constituents of the internals of the cell but approximates the response that can be measured at the terminals under a specified test condition. Externally, this can be viewed as the potential across V_{AB}, as shown in Figure 2, imposing the same conditions on current, voltage, and temperature. The electrical passive and active components of the circuit are what is to be modeled in MATLAB/Simulink. A custom "grey box" circuit element is added in series that approximates the unexplained portion of the model not fully captured by simple capacitor-resistor combinations. Assume that this custom component has a hysteresis voltage V_h and a hysteresis time constant τ_h.

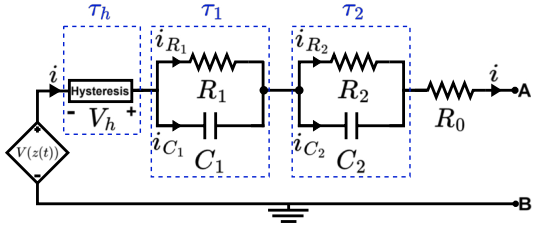

Figure 2. This 2RC ECM includes the minimum necessary components to accurately describe the observed response under constant temperature.

In this regard, the discrete state space equations of a 2^{nd} order model can be defined for parameter identification:

$$\begin{bmatrix} z(k+1) \\ i_{R_1}(k+1) \\ i_{R_2}(k+1) \\ h(k+1) \end{bmatrix} = \begin{bmatrix} 1 & 0 & 0 & 0 \\ 0 & \tau_1 & 0 & 0 \\ 0 & 0 & \tau_2 & 0 \\ 0 & 0 & 0 & \tau_h \end{bmatrix} \begin{bmatrix} z(k) \\ i_{R_1}(k) \\ i_{R_2}(k) \\ h(k) \end{bmatrix} + \begin{bmatrix} \Delta t/Q & 0 \\ 1-\tau_1 & 0 \\ 1-\tau_2 & 0 \\ 0 & 1-\tau_h \end{bmatrix} \begin{bmatrix} i(k) \\ \text{sgn}(i(k)) \end{bmatrix} \tag{2}$$

$$v(k) = OCV_{avg}(z(k)) + OCV_h(z(k)) \cdot h(k) + R_1 \cdot i_{R_1}(k) + R_2 \cdot i_{R_2}(k) + R_0 \cdot i(k) \tag{3}$$

z denotes the capacity, i_{R1} and i_{R2} denote the current passing through the resistors in the parallel RC pairs. h is the hysteresis voltage state. i is the battery current, and $sgn(i)$ is the sign of the current. τ_1 and τ_2, and τ_h are time constants of the parallel RC pairs and hysteresis given by:

$$\tau_1 = \exp\left(-\frac{\Delta t}{R_1 \cdot C_1}\right),\ \tau_2 = \exp\left(-\frac{\Delta t}{R_2 \cdot C_2}\right),\ \tau_h = \exp\left(-\left|\frac{i(k) \cdot \gamma \cdot \Delta t}{Q}\right|\right) \tag{4}$$

Unlike polarization potential which can be captured by capacitor time constants τ_1 and τ_2, hysteresis is dependent on current direction and SOC, interpreted as dz. The OCV trajectory for a given charge or discharge cycle is tuned by the newly identified state parameter γ, which is a variable positive scalar. The purpose of this parameter is to adjust the trajectory of the OCV between bounds of maximum and minimum hysteresis M; this parameter is defined as a function of SOC and rate of change of SOC. The difference between M and the hysteresis voltage h provides the distance away from major loop bounds defined by the maximum of M for charge or discharge. The mathematical interpretation as a constant scalar for SOC is further detailed in the work by (Plett, 2015) and is implemented variably for SOC in the proceeding forms. The continuous form of the hysteresis equation is defined as follows and can be implemented into Simulink with some further modifications:

$$\frac{dh(z,t)}{dz} = \gamma\, sgn(\dot{z})(M(z,\dot{z}) - h(z,t)) \tag{5}$$

This equation describes the observable characteristic as it varies with SOC. To further simplify this equation, it is reduced to a form that can be directly modeled by Simulink with readily available blocks:

$$\dot{h}(t) = -\left|\frac{\eta(t)i(t)\gamma}{Q}\right| h(t) + \left|\frac{\eta(t)i(t)\gamma}{Q}\right| \cdot sgn(i[k]) \tag{6}$$

where,

$$M(z,\dot{z}) = -M \cdot sgn(i[k]) \tag{7}$$

For implementation, a discrete-time version of (6) is given by:

$$h[k+1] = \exp\left(-\left|\frac{\eta[k]i[k]\gamma\, t}{Q}\right|\right) h[k] - \left(1 - \exp\left(-\left|\frac{\eta[k]i[k]\gamma\, t}{Q}\right|\right)\right) \cdot sgn(i[k]) \tag{8}$$

such that dynamic hysteresis voltage V_h is:

$$V_h[k+1] = M \cdot h[k] \tag{9}$$

(9) is the dynamic hysteresis term to be included in the total hysteresis voltage equation defined by both dynamic and instantaneous parts in (11). This description of a dynamic and instantaneous part was originally described in (Ewing, 1885). The constant terms were implemented in (Plett, 2015). The instantaneous hysteresis is modeled as:

$$s[k] = \begin{cases} sgn(i[k]), & |i[k]| > 0; \\ s[k-1], & \text{otherwise.} \end{cases} \tag{10}$$

$s[k]$ is set such that the state of the systems is charging or discharging. Holding the previous state: when $i[k] = 0$, the system maintains its previous state. Then, the total hysteresis voltage can be described as:

$$V_h = M_0 s[k] + Mh[k] \tag{11}$$

Where M_0 is also a tunable parameter. The total hysteresis voltage equation models both immediate and historical dependencies.

4. ECM CALIBRATION METHOD

The ECM calibration was performed for each HNTC cell sample (for a total of six cells). Cell data was obtained from various lab tests to be used in the ECM calibration for characterizing the OCV-SOC, identification of ECM parameters and validation of the model.

Obtaining the OCV is done using a thermal chamber and cycler. Measurements on the cell terminals are done at equilibrium points, after sufficient rest times, and interpolated during ECM calibration for a predefined number of SOC points. After characterizing the OCV, the separate charge and discharge ECM parameters, R_0, R_1, R_2, τ_1, τ_2, and combined charge and discharge hysteresis parameters, τ_h, M_0, are obtained from a hybrid pulse power characterization (HPPC) test for 15 SOC breakpoints and interpolated linearly. The test conditions may be modified, but the standardized procedures can be consulted in (Christophersen, 2015).

OCV points are captured before and after current pulses to be used in the optimization of the cost function. The identification was performed with bounds that allow enough degrees of freedom for the solver to find the minimum voltage error while avoiding saturation of parameter values. The maximum bounds for γ are 0.5 to 600, and the bounds for M_0 are defined for 0 to 175mV. The values of the sample level γ and M_0 are new parameters identified for $x[k]$ to accommodate dynamic hysteresis and total, dynamic plus instantaneous, hysteresis modeling.

The models were validated with and without hysteresis descriptions. The virtual model imposes the same experimental conditions as the samples tested in the laboratory. The accuracy of the ECM is measured using repeated Worldwide Harmonised Light Vehicles Test Procedure (WLTP) cycles. Capturing a variety of dynamic conditions the cells may be subjected to in an EV environment. The accuracy is reported as a root mean square error (RMSE). The RMSE is a measure of difference between the true response of the cell and the model's response under the same conditions. The model response was tested for 2RC (benchmark model with no hysteresis), 2RCh (including dynamic hysteresis), and 2RCh0 (including dynamic and instantaneous hysteresis). The RMSE is reported for several SOC windows.

To inspect the response of a variable tuning rate for the prescribed SOC regions of each sample and temperature, an analysis by ANCOVAN was performed. This analysis is robust to non-parametric responses and large datasets (Olejnik and Algina, 1984). This was tested for 1RC and 2RC hysteresis models where the hysteresis voltage factor is included as well as its interaction with the SOC. Two hypotheses are stipulated based on the test data included in the analysis dataset. The resulting p value is monitored. A standard threshold of $\alpha = 0.05$ was selected. Where, a value of p exceeding 0.05 is considered not to be a statistical significance to the response of γ. Considering that the hysteresis model is to be applied for SOC regions possessing large hysteresis errors, the 0-50% SOC region is promptly investigated.

5. RESULTS AND DISCUSSION

5.1 Open Circuit Voltage Characteristic

Obtaining the OCV-SOC characteristic was the first objective of the calibration process. This was obtained by combining the OCV measurements made at equilibrium points for both charge and discharge cycles. The multi-temperature results of the characteristic are shown in Figure 3. The corresponding hysteresis voltage for the major loop is also shown in Figure 3. This was done for all six samples of the subject cell. The hysteresis voltage is taken as a difference between the maximum and minimum OCV. It was determined that the maximum hysteresis voltage was 69mV at 5% SOC, with comparatively low hysteresis voltage magnitudes occurring after 50% SOC.

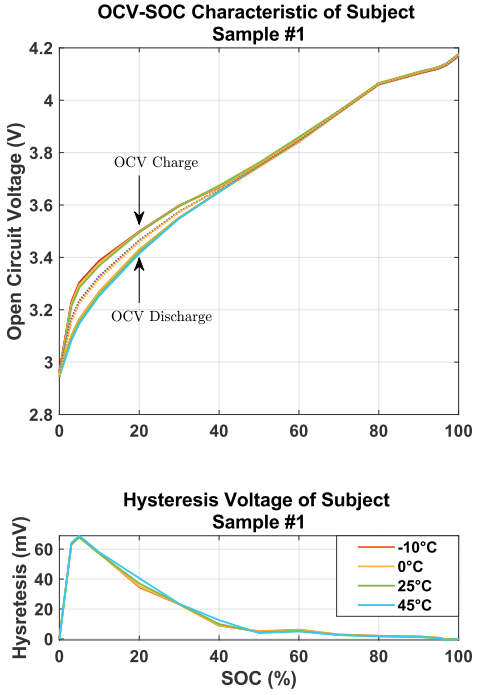

Figure 3. The charge and discharge OCV-SOC characteristic of subject sample #1 and its major hysteresis voltage profile. Each color denotes a temperature, and the mean OCV approximation is represented by a dotted line.

5.2 Variable Tuning Rate Identification

To identify the ECM parameters featured in the model seen in Figure 2, constrained nonlinear optimization was performed for all ECM calibrations. This was done to minimize the objective function while satisfying the constraints. The identification of the model parameters required an HPPC test procedure. The response of the variable tuning rate of the 2RCh model (denoted as γ_2) is shown in Figure 4. The hysteresis profile is also plotted to demonstrate the variable tuning rate's response in the regions with and without large hysteresis voltages. The mean magnitude of γ_2 is inversely proportional to the temperature and increases non-linearly. This suggests that a more aggressive tuning (shorter mean τ_h) is necessary in the model's estimation of the OCV at lower temperatures.

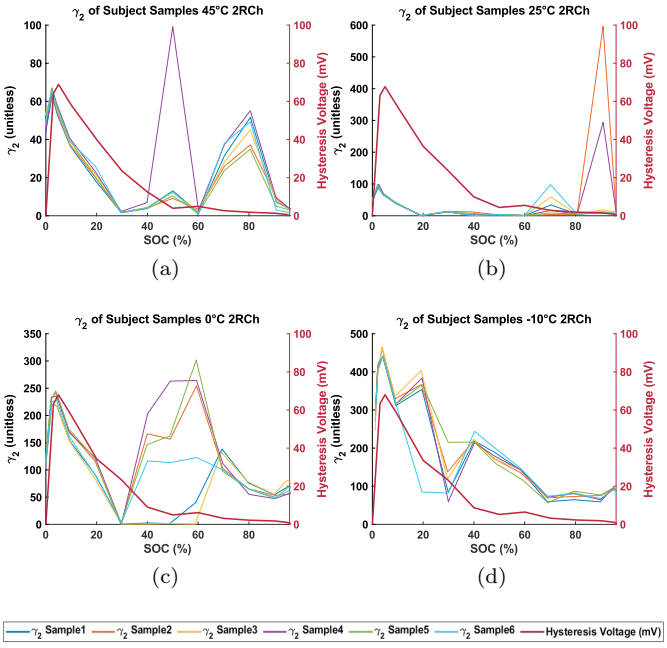

Figure 4. The response of γ_2 in the 2RCh model for each sample and temperature.

5.3 Validation of the Model

Considering that the most significant hysteresis errors are observed in Figure 3 from 0-50% SOC, the corresponding RMSE is captured. The overall performance is captured for 0-100% SOC, and the 50-100% SOC region with low hysteresis errors is recorded as well. This was done for each of the four temperatures. The 2RC model accuracies are shown in Figure 5 (a). The same conditions were tested for the equivalent subset of 1RC models and is shown in Figure 5 (b). Adding any description of hysteresis improves the model accuracy under a WLTP cycle for all 2-96% windows. Across all temperatures, the 1RC models have improvements of 7-32%, while 2RC models have the greatest improvements of 16-33%. Generally, the error reduction was more significant for higher temperatures for up to 33% reduction. In some instances, adding instantaneous hysteresis made the model perform worse in both 1RC and 2RC models compared to just dynamic models. In the 1RC models, adding instantaneous hysteresis increases the error by up to 2.14%, seen for a 50-96% SOC window. In 2RC models, adding instantaneous hysteresis increases the error by up to 4.72%, seen for a 2-50% SOC window. It is also noted that the improvements at low SOC regions for HNTC cells are predictive of the full SOC range ECM performance. This finding suggests that model selection is appropriate when validating under dynamic cycles in the 0-50% SOC range.

5.4 Analysis of Covariance of the Tuning Rate

The summarized results of the analysis are shown in Table 1 and Table 2 for each SOC window selected. The p value results after performing ANCOVAN for the response of γ to a single factor (exclusively hysteresis voltage) is shown in Table 1. The two factor interaction (between hysteresis voltage *and* SOC) results are shown in Table 2. It can

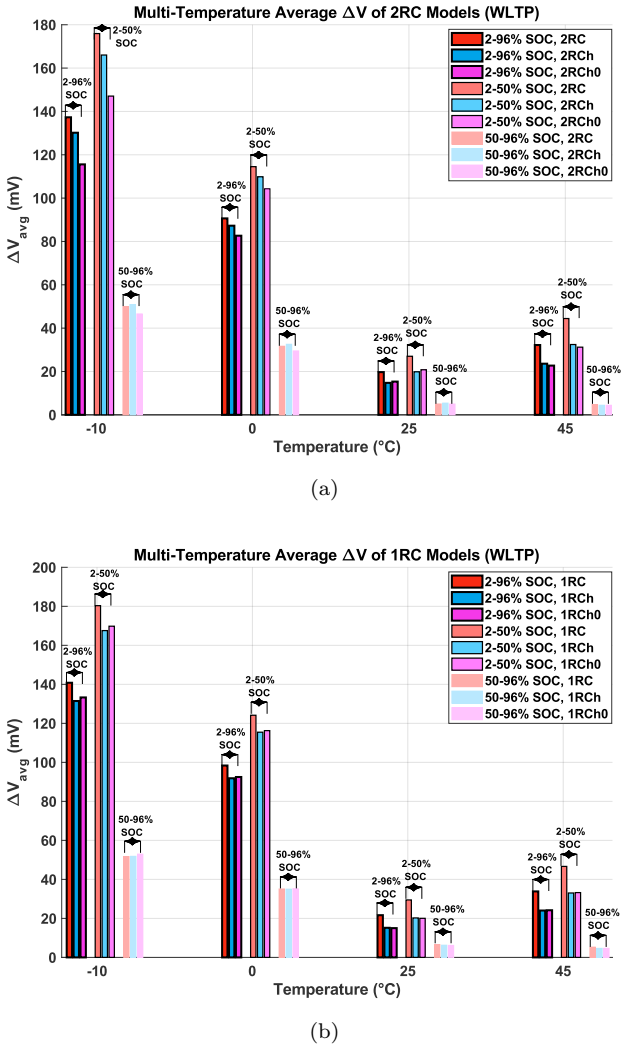

Figure 5. The validation results of (a) 2RC and (b) 1RC models for 45°C, 25°C, 0°C, and -10°C. Separated for SOC windows of 2-50% SOC, 50-96% SOC, and 2-96% SOC. Average modeling error (ΔV_{avg}) including hysteresis descriptions are lower in call cases compared to the benchmark model for 2-96% SOC.

be seen in Table 1, that p values corresponding to the 0-50% SOC region are statistically significant for all models, except for 1RCh0. Comparatively to dynamic hysteresis models, the p values of models including instantaneous hysteresis descriptions are not truly zero. Where, the statistical significance of hysteresis voltage on a variable γ response is generally less significant or not significant at all for instantaneous modeling. Table 2 on the other hand, analyzes the interaction of the hysteresis voltage and SOC factors on the variable γ response. It is seen that only for the 0-50% SOC window there is statistical significance considering both factors for *all* models and temperatures tested. Hence, SOC windows with large hysteresis bounds in their OCV-SOC characteristic are statistically significant to a variable tuning rate for parameter identification in ECMs. This finding suggests a variable tuning rate is best suited for the low SOC regions of HNTC cells. The results of this test are exclusive to the HNTC subject samples tested. For better statistical power of this analysis,

Table 1. Summary of p Values Observing Hysteresis Voltage

SOC:	0-100%		0-50%		50-100%	
Model	1RCh	1RCh0	1RCh	1RCh0	1RCh	1RCh0
P value	**0**	**0.1718**	**0**	**0.3565**	**0.0023**	**0.9752**
Model	2RCh	2RCh0	2RCh	2RCh0	2RCh	2RCh0
P value	**0**	**0.0545**	**0**	**0.0153**	**0.1081**	**0.7814**

Table 2. Summary of p Values Observing Hysteresis Voltage & SOC Interaction

SOC:	0-100%		0-50%		50-100%	
Model	1RCh	1RCh0	1RCh	1RCh0	1RCh	1RCh0
P value	**0**	**0.0004**	**0**	**0.0161**	**0.0021**	**0.956**
Model	2RCh	2RCh0	2RCh	2RCh0	2RCh	2RCh0
P value	**0**	**0.0924**	**0**	**0.0204**	**0.0537**	**0.6563**

it is recommended to have a larger dataset including cells with different capacities and chemistry.

6. CONCLUSIONS

In this work, an accurate ECM including a hysteresis one-state model was applied to the battery ECM framework for HNTC cells. A variable tuning rate (gamma), for both 1RC and 2RC models was investigated. The model accuracy was validated under dynamic conditions using a WLTP cycle. Improvements to select models are demonstrated for specified SOC windows and temperatures. The statistical significance of hysteresis voltage to a gamma for dynamic and total hysteresis models was inspected. By including a mathematical model to address hysteresis directly, improvements to the ECM accuracy for HNTC cells under a WLTP cycle are proven. Accuracy improvements of 7-32% for 1RC models and 16-33% for 2RC models are achieved in a 2-96% SOC range. Validation also demonstrated that the ECM performance for the 0-50% SOC regions is indicative of the full capacity performance for 2-96% SOC. Using ANCOVAN, it is determined that SOC windows with large hysteresis bounds in their OCV-SOC characteristic are statistically significant to a variable tuning rate, γ, for parameter identification in Thevenin-based battery ECMs. This suggests that a variable tuning rate is best suited for low SOC regions of HNTC cells. The accuracy of the ECM including an instantaneous hysteresis description is dependent on the model order and is statistically insignificant to the measured hysteresis voltage alone. This suggests that a suitable one-state model should be selected based on order and temperature. These results are specific to the cell samples tested, however, the methodology can be extended to any cell within the calibration framework. Future works intend to include 3RC models, different cells, chemistry, and capacities.

REFERENCES

Akhilash, M., Salini, P.S., John, B., and Mercy, T.D. (2021). A journey through layered cathode materials for lithium ion cells. *Journal of Alloys and Compounds*, 869, 159–239.

Anton Van der Ven, Kimberly A. See, L.P. (2022). Hysteresis in electrochemical systems. *Battery Energy*, 1, 20210017.

Biju, N. and Fang, H. (2023). On the design of an equivalent circuit model for lithium-ion batteries operating across broad current ranges. *IFAC-PapersOnLine*, 56, 7127–7133.

Chayratsami, P. and Plett, G.L. (2019). Hysteresis modeling of lithium–silicon half cells using krasnosel'skii-pokrovskii model. In *2019 IEEE Conference on Control Technology and Applications (CCTA)*, 470–475.

Cheng, H., Shapter, J.G., Li, Y., and Gao, G. (2021). Recent progress of advanced anode materials of lithium-ion batteries. *Journal of Energy Chemistry*, 57, 451–468.

Christophersen, J.P. (2015). Battery test manual for electric vehicles, revision 3. Technical report, Idaho National Lab. (INL), Idaho Falls, ID (United States).

Ewing, J.A. (1885). Experimental researches in magnetism. *Philosophical Transactions of the Royal Society of London*, 176, 523–640.

Hassani, V., Tjahjowidodo, T., and Do, T.N. (2014). A survey on hysteresis modeling, identification and control. *Mechanical Systems and Signal Processing*, 49.

Hodakovska, J., Britala, L., Mezulis, A., Grinberga, L., Bajars, G., and Kucinskis, G. (2024). State of health as a function of voltage hysteresis in li-ion battery half-cells. *Journal of Solid State Electrochemistry*.

Lin, C., Yu, Q., Xiong, R., and Wang, L.Y. (2017). A study on the impact of open circuit voltage tests on state of charge estimation for lithium-ion batteries. *Applied Energy*, 205, 892–902.

Lipu, M.S.H., Hannan, M.A., Karim, T.F., Hussain, A., Saad, M.H.M., Ayob, A., Miah, M.S., and Mahlia, T.M.I. (2021). Intelligent algorithms and control strategies for battery management systems. *Journal of Cleaner Production*, 292, 126044.

Murdock, B.E., Toghill, K.E., and Tapia-Ruiz, N. (2021). A perspective on the sustainability of cathode materials used in lithium-ion batteries. *Advanced Energy Materials*, 11, 2102028.

Naseri, F., Schaltz, E., Stroe, D.I., Gismero, A., and Farjah, E. (2022). An enhanced equivalent circuit model with real-time parameter identification for battery state-of-charge estimation. *IEEE Transactions on Industrial Electronics*, 69, 3743–3751.

Nozarijouybari, Z. and Fathy, H.K. (2024). Test trajectory optimization for parameterizing a neural network-based equivalent circuit battery model. *IFAC-PapersOnLine*, 58, 198–203.

Olejnik, S.F. and Algina, J. (1984). Parametric ancova and the rank transform ancova when the data are conditionally non-normal and heteroscedastic. *Journal of Educational Statistics*, 9, 129–149.

Plett, G.L. (2015). *Battery Management Systems, Volume I: Battery Modeling*. Artech House.

Plett, G.L. (2004). Extended kalman filtering for battery management systems of lipb-based hev battery packs: Part 2. modeling and identification. *Journal of Power Sources*, 134, 262–276.

Tekin, M. and Karamangil, M.I. (2024). Comparative analysis of equivalent circuit battery models. *Journal of Energy Storage*, 86, 111327.

Tran, M.K., Mathew, M., Janhunen, S., Panchal, S., Raahemifar, K., Fraser, R., and Fowler, M. (2021). A comprehensive equivalent circuit model for lithium-ion batteries. *Journal of Energy Storage*, 43, 103252.

Whittingham, M.S. (2019). The origins of the lithium battery. *The Nobel Prizes*, 184–201.